PAPER

Equivalent-Circuit Model with Retarded Electromagnetic Coupling for Meta-Atoms of Wired Metallic Spheres

Katsuya OHISHI[†], ***Student Member***, **Takashi HISAKADO**[†a)], **Tohlu MATSUSHIMA**[†], ***Members***, ***and*** **Osami WADA**[†], ***Fellow***

SUMMARY This paper describes the equivalent-circuit model of a metamaterial composed of conducting spheres and wires. This model involves electromagnetic coupling between the conductors, with retardation. The lumped-parameter equivalent circuit, which imports retardation to the electromagnetic coupling, is developed in this paper from Maxwell's equation. Using the equivalent-circuit model, we clarify the relationship between the retardation and radiation loss; we theoretically demonstrate that the electromagnetic retardation in the near-field represents the radiation loss of the meta-atom in the far-field. Furthermore, this paper focuses on the retarded electromagnetic coupling between two meta-atoms; we estimate the changes in the resonant frequencies and the losses due to the distance between the two coupled meta-atoms. It is established that the dependence characteristics are significantly affected by electromagnetic retardation.

key words: *metamaterial, meta-atom, equivalent-circuit model, retardation, radiation, electromagnetic coupling*

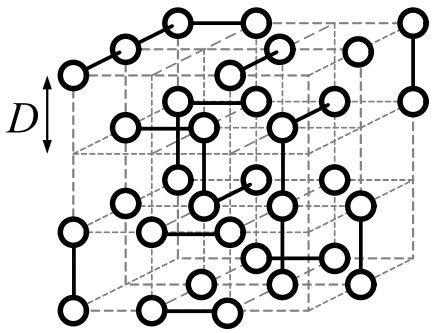

Fig. 1 Wired Metallic Spheres [9].

1. Introduction

Electromagnetic metamaterials are structures composed of meta-atoms made of metals or dielectrics and produce artificial electromagnetic phenomena; the analyses of these phenomena are highly complex and difficult because of the complexity of their structures. To overcome this difficulty, equivalent-circuit models are used. These models render the analysis easy and enable the understanding of the metamaterial-phenomena, with respect to the circuit models and theoretical discussion on these phenomena [1]–[7].

The partial element equivalent circuit (PEEC) [8] is a well-known equivalent-circuit model theoretically derived from Maxwell's equation. Although the method provides full-wave analysis for general structures, it requires many circuit elements because it is based on mesh division. On the other hand, the equivalent-circuit model proposed by [9] focuses on the structures of the wired metallic spheres [10], as shown in Fig. 1 and derives a simple equivalent-circuit model, which has the same topology as that of the wires. Although the equivalent-circuit model is derived from near-field coupling, the model expresses the radiation from the meta-atoms through the radiation resistance calculated at far-field. In order to obtain a more consistent model, a new model without radiation resistance is required.

We propose a consistent equivalent-circuit model for the wired metallic spheres by evaluating the electromagnetic retardation between the conductors. The retardation for the circuit model was introduced in [11], and discussed in the EIT and the transmission line, in addition [12], [13]. Furthermore, the relationship between the radiation loss, energy consumption, and retardation is discussed in [14], [15]. However, these examples are full-wave analyses and discuss the retardation effects using only the results of simulation with many meshes.

Using a consistent equivalent circuit with retardation for a simple meta-atom, we demonstrate that the inductance and potential coefficients are represented by complex numbers. Then, we theoretically estimate the loss described by the real part of the impedances based on the retardation, using the Taylor expansion. The results show that the representation of the loss by the retardation corresponds to the radiation loss based on the far-field. Further, we discuss the retarded coupling between meta-atoms with respect to the natural angular frequencies and loss. We derive their dependence due to the distance between the meta-atoms and demonstrate that the characteristics of the dependence are significantly affected by retardation.

This paper is organized as follows: In Sect. 2, we introduce the equivalent-circuit equation of a metamaterial composed of wired metallic spheres, considering the retardation between the conductors. In Sect. 3, we compare the loss in the equivalent-circuit equation generated by the retardation with the radiation resistance of a meta-atom. In Sect. 4, we analyze the effect of retardation on the natural angular frequencies using the proposed model. Further, we compare the results of the proposed model with the electromagnetic-field analysis. In Sect. 5, we conclude the paper.

Manuscript received September 25, 2017.
Manuscript revised July 9, 2018.
[†]The authors are with Department of Electrical Engineering, Kyoto University, Kyoto-shi, 615–8510 Japan.
a) E-mail: hisakado@kuee.kyoto-u.ac.jp
DOI: 10.1587/transele.E101.C.923

2. Equivalent-Circuit Equation with Retardation

2.1 Spatial Discretization

We review the spatial discretization of the wired metallic spheres of the perfect conductor proposed in [9]. We discretize the current and charge using bases defined on the central axis of the wire and on the center of the sphere, respectively; an example with wired metallic spheres is shown in Fig. 2. D is the length between the centers of two spheres. The radii of the wire and sphere are denoted by a and b, respectively. If λ is defined as the wavelength of the incident wave, we assume that these parameters satisfy $a \ll b \ll D \ll \lambda$; we approximate that the charges exist on the centers of the spheres and the current exists along the central axes of the wires with a uniform distribution, except for the estimation of self-interactions such as the self-inductance and self-capacitance. Denoting the bases of current in the n-th wire and charge on the m-th sphere by $\boldsymbol{\Psi}_n$ and Φ_m, respectively [9], we can express the current and charge densities as

$$\begin{aligned} \boldsymbol{J}(\boldsymbol{r},t) &= \sum_n I_n(t)\boldsymbol{\Psi}_n(\boldsymbol{r}), \\ \rho(\boldsymbol{r},t) &= \sum_m Q_m(t)\Phi_m(\boldsymbol{r}), \end{aligned} \tag{1}$$

where I_n is the current in the n-th wire, and Q_m is the charge on the m-th sphere. The bases, $\boldsymbol{\Psi}_n(\boldsymbol{r})$ and $\Phi_m(\boldsymbol{r})$, correspond to the wire and sphere, respectively. The functions, $\boldsymbol{\Psi}_n(\boldsymbol{r})$ and $\Phi_m(\boldsymbol{r})$, are related as follows:

$$\nabla \cdot \boldsymbol{\Psi}_n(\boldsymbol{r}) = \sum_m U_{mn}\Phi_m(\boldsymbol{r}), \tag{2}$$

where U_{mn} is the incident matrix. Then, the current continuity equation is given by

$$\sum_n U_{mn}I_n(t) + \frac{\partial}{\partial t}Q_m(t) = 0. \tag{3}$$

We use the basis, $\boldsymbol{\Psi}_n(\boldsymbol{r})$, as a test function, except for the self-interactions. When considering a self-interaction, we use a test function, $\boldsymbol{\Psi}^{\mathrm{S}}_n(\boldsymbol{r})$, defined on the surface of a wire. A simple example depicting the locations of the test functions is shown in Fig. 3. Similarly, we use the basis, $\Phi_m(\boldsymbol{r})$, as a test function, except for self-interactions. When considering the self-interaction of a charge, a test function, $\Phi^{\mathrm{S}}_m(\boldsymbol{r})$, defined on the surface of the sphere is used. The test functions, $\boldsymbol{\Psi}^{\mathrm{W}}_n(\boldsymbol{r})$ and $\Phi^{\mathrm{W}}_m(\boldsymbol{r})$, are summarized as follows:

$$\boldsymbol{\Psi}^{\mathrm{W}}_n(\boldsymbol{r}) = \begin{cases} \boldsymbol{\Psi}^{\mathrm{S}}_n(\boldsymbol{r}) & (n = n') \\ \boldsymbol{\Psi}_n(\boldsymbol{r}) & (n \neq n'), \end{cases} \tag{4}$$

$$\Phi^{\mathrm{W}}_m(\boldsymbol{r}) = \begin{cases} \Phi^{\mathrm{S}}_m(\boldsymbol{r}) & (m = m') \\ \Phi_m(\boldsymbol{r}) & (m \neq m'). \end{cases} \tag{5}$$

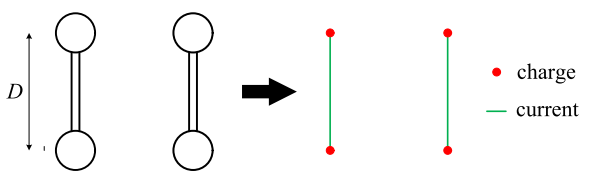

Fig. 2 Discretization example. The charges exist on the centers of the spheres and the currents exist along the central axes of the wires.

2.2 Circuit Equation with Retardation

The equivalent-circuit equation of a structure excited by an incident electric field, $\boldsymbol{E}^{\mathrm{E}}(\boldsymbol{r},t)$, is introduced by the boundary condition [9] as

$$\begin{aligned} &\sum_{n'} \frac{\partial}{\partial t} \int \bar{L}_{nn'}(t,t')I_{n'}(t')\mathrm{d}t' \\ &\quad - \sum_{m'}\sum_{m} \int U_{mn}\bar{P}_{mm'}(t,t')Q_{m'}(t')\mathrm{d}t' = -V^{\mathrm{E}}_n(t), \end{aligned} \tag{6}$$

where

$$\begin{aligned} &\bar{L}_{nn'}(t,t') \\ &\quad = \mu_0 \int_V \int_{V'} \boldsymbol{\Psi}^{\mathrm{W}}_n(\boldsymbol{r})G(\boldsymbol{r},t,\boldsymbol{r}',t')\boldsymbol{\Psi}_{n'}(\boldsymbol{r}')\mathrm{d}^3\boldsymbol{r}'\mathrm{d}^3\boldsymbol{r}, \end{aligned} \tag{7}$$

$$\begin{aligned} &\bar{P}_{mm'}(t,t') \\ &\quad = \frac{1}{\varepsilon_0} \int_V \int_{V'} \Phi^{\mathrm{W}}_m(\boldsymbol{r})G(\boldsymbol{r},t,\boldsymbol{r}',t')\Phi_{m'}(\boldsymbol{r}')\mathrm{d}^3\boldsymbol{r}'\mathrm{d}^3\boldsymbol{r}, \end{aligned} \tag{8}$$

$$V^{\mathrm{E}}_n(t) = -\int_{\mathrm{V}} \boldsymbol{\Psi}^{\mathrm{W}}_n(\boldsymbol{r})\boldsymbol{E}^{\mathrm{E}}(\boldsymbol{r},t)\mathrm{d}^3\boldsymbol{r}. \tag{9}$$

The function, $G(\boldsymbol{r},t,\boldsymbol{r}',t')$, is the Green's function, expressed as

$$G(\boldsymbol{r},t,\boldsymbol{r}',t') = \frac{\delta(t-t'-\frac{|\boldsymbol{r}-\boldsymbol{r}'|}{c})}{4\pi|\boldsymbol{r}-\boldsymbol{r}'|}, \tag{10}$$

where $\frac{|\boldsymbol{r}-\boldsymbol{r}'|}{c}$ is the retardation between the locations of the basis and the test functions. If we neglect the retardation of the Green's function, the Green's function is approximated by

$$G(\boldsymbol{r},t,\boldsymbol{r}',t') = \frac{\delta(t-t')}{4\pi|\boldsymbol{r}-\boldsymbol{r}'|}, \tag{11}$$

which is used in [9]. We import the concept of retarded electromagnetic coupling given by Eq. (10), instead of that

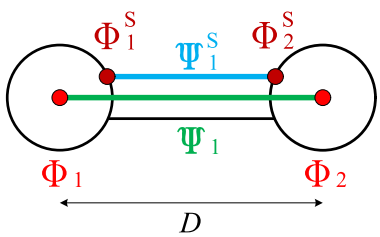

Fig. 3 Locations of the base and test functions. Only the self-interaction test functions are located on the surfaces of the structures.

given by Eq. (11).

Next, we treat the equivalent-circuit equation in the frequency domain. The operation of the delta function in Eq. (10) indicates that the electromagnetic retardation is depicted in the frequency domain as the factor of

$$\exp\left(-\mathrm{j}\omega\frac{|\boldsymbol{r}-\boldsymbol{r'}|}{c}\right). \tag{12}$$

From Eqs. (3) and (6), the equivalent-circuit equation with retardation is given by

$$(-\omega^2\mathbf{1}+\hat{\boldsymbol{L}}^{-1}\boldsymbol{U}^{\mathrm{T}}\hat{\boldsymbol{P}}\boldsymbol{U})\boldsymbol{I}(\omega)=-\mathrm{j}\omega\hat{\boldsymbol{L}}^{-1}\boldsymbol{V}^{\mathrm{E}}(\omega), \tag{13}$$

where $\boldsymbol{U}$ is the incident matrix; matrices $\hat{\boldsymbol{L}}$ and $\hat{\boldsymbol{P}}$, and vector, $\boldsymbol{V}^{\mathrm{E}}(\omega)$, are represented by

$$\hat{L}_{nn'}(\omega) = \mu_0\int_V\int_{V'}\boldsymbol{\Psi}_n^{\mathrm{W}}(\boldsymbol{r})\frac{\exp(-\mathrm{j}\omega\frac{|\boldsymbol{r}-\boldsymbol{r'}|}{c})}{4\pi|\boldsymbol{r}-\boldsymbol{r'}|}\boldsymbol{\Psi}_{n'}(\boldsymbol{r})\mathrm{d}^3\boldsymbol{r'}\mathrm{d}^3\boldsymbol{r}, \tag{14}$$

$$\hat{P}_{mm'}(\omega) = \frac{1}{\varepsilon_0}\int_V\int_{V'}\Phi_m^{\mathrm{W}}(\boldsymbol{r})\frac{\exp(-\mathrm{j}\omega\frac{|\boldsymbol{r}-\boldsymbol{r'}|}{c})}{4\pi|\boldsymbol{r}-\boldsymbol{r'}|}\Phi_{m'}(\boldsymbol{r'})\mathrm{d}^3\boldsymbol{r'}\mathrm{d}^3\boldsymbol{r}, \tag{15}$$

$$V_n^{\mathrm{E}}(\omega) = -\int_{\mathrm{V}}\boldsymbol{\Psi}_n^{\mathrm{W}}(\boldsymbol{r})\boldsymbol{E}^{\mathrm{E}}(\boldsymbol{r},\omega)\mathrm{d}^3\boldsymbol{r}. \tag{16}$$

It is to be noted that the components, $\hat{L}_{nn'}$ and $\hat{P}_{mm'}$, are expressed by complex numbers.

3. Relationship between Retardation and Radiation Loss

3.1 Real Part of the Impedance with Retardation

Using a simple meta-atom, which we call an I-shaped meta-atom, as shown in Fig. 4, we discuss the relationship between the retardation and radiation loss. Matrices $\hat{\boldsymbol{L}}$ and $\hat{\boldsymbol{P}}$ in Eq. (13) are expressed as

$$\hat{\boldsymbol{L}}=\left[\hat{L}\right],\quad \hat{\boldsymbol{P}}=\begin{bmatrix}\hat{P}_{11} & \hat{P}_{12}\\ \hat{P}_{21} & \hat{P}_{22}\end{bmatrix}=\frac{1}{4\pi\varepsilon_0}\begin{bmatrix}\frac{\exp(-\mathrm{j}\omega\frac{b}{c})}{b} & \frac{\exp(-\mathrm{j}\omega\frac{D}{c})}{D}\\ \frac{\exp(-\mathrm{j}\omega\frac{D}{c})}{D} & \frac{\exp(-\mathrm{j}\omega\frac{b}{c})}{b}\end{bmatrix}. \tag{17}$$

Component, $\hat{L}$, is the self-inductance and is expressed as

$$\hat{L}=\frac{\mu_0}{4\pi}\int_b^{D-b}\int_0^D\frac{\cos(\omega\frac{\sqrt{(z-z')^2+a^2}}{c})}{\sqrt{(z-z')^2+a^2}}\mathrm{d}z'\mathrm{d}z$$

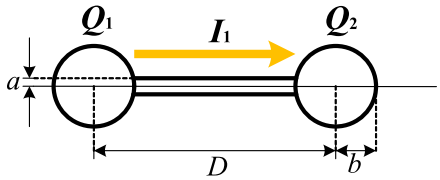

Fig. 4 I-shaped meta-atom

$$-\mathrm{j}\frac{\mu_0}{4\pi}\int_0^D\int_0^D\frac{\sin(\omega\frac{\sqrt{(z-z')^2+a^2}}{c})}{\sqrt{(z-z')^2+a^2}}\mathrm{d}z'\mathrm{d}z. \tag{18}$$

The calculation details of $\hat{L}$ are presented in Appendix A. The incident matrix, $\boldsymbol{U}$, is expressed as

$$\boldsymbol{U}=\begin{bmatrix}1\\-1\end{bmatrix}. \tag{19}$$

Instead of Eq. (13), we discuss the equivalent equation,

$$\left(\mathrm{j}\omega\hat{\boldsymbol{L}}+\frac{\boldsymbol{U}^{\mathrm{T}}\hat{\boldsymbol{P}}\boldsymbol{U}}{\mathrm{j}\omega}\right)\boldsymbol{I}(\omega)=-\boldsymbol{V}^{\mathrm{E}}(\omega). \tag{20}$$

From Eqs. (17) and (19), Eq. (20) is represented by

$$\left(\mathrm{j}\omega\hat{L}+2\frac{\hat{P}_{11}-\hat{P}_{12}}{\mathrm{j}\omega}\right)I_1(\omega)=-V_1^{\mathrm{E}}(\omega). \tag{21}$$

Here, we define an impedance, Z, by

$$Z\equiv\mathrm{j}\omega\hat{L}+2\frac{\hat{P}_{11}-\hat{P}_{12}}{\mathrm{j}\omega}. \tag{22}$$

Because components $\hat{L}$, $\hat{P}_{11}$, and $\hat{P}_{12}$ are expressed as complex numbers, we define the real and the imaginary parts by

$$\hat{L}=L^{\mathrm{r}}+\mathrm{j}L^{\mathrm{j}},\quad \hat{P}_{11}=P_{11}^{\mathrm{r}}+\mathrm{j}P_{11}^{\mathrm{j}},\quad \hat{P}_{12}=P_{12}^{\mathrm{r}}+\mathrm{j}P_{12}^{\mathrm{j}}. \tag{23}$$

Then, Z^{r}, which is the real part of Z, is expressed as

$$Z^{\mathrm{r}}=-\omega L^{\mathrm{j}}+2\frac{P_{11}^{\mathrm{j}}-P_{12}^{\mathrm{j}}}{\omega}. \tag{24}$$

The real part, which expresses the loss in the equivalent circuit, consists of the imaginary parts of the inductance and capacitances generated by the retardation.

3.2 Comparison of Z^{r} with the Radiation Resistance

We evaluate Z^{r} using the Taylor expansion. Components L^{j}, P_{11}^{j}, and P_{12}^{j} are expressed as

$$\begin{aligned}L^{\mathrm{j}}&=-\frac{\mu_0}{4\pi}\int_0^D\int_0^D\frac{\sin(\omega\frac{\sqrt{(z-z')^2+a^2}}{c})}{\sqrt{(z-z')^2+a^2}}\mathrm{d}z'\mathrm{d}z\\&=-\frac{\mu_0}{4\pi}\int_0^D\int_0^D\left\{\frac{\omega}{c}-\frac{(z-z')^2+a^2}{3!c^3}\omega^3+\cdots\right\}\mathrm{d}z'\mathrm{d}z\\&=-\frac{\mu_0}{4\pi}\left\{\frac{D^2}{c}\omega-\frac{1}{3!c^3}\left(\frac{1}{6}D^4+D^2a^2\right)\omega^3+\cdots\right\},\end{aligned} \tag{25}$$

$$\begin{aligned}P_{11}^{\mathrm{j}}&=-\frac{\sin(\omega\frac{b}{c})}{4\pi\varepsilon_0 b}\\&=-\frac{1}{4\pi\varepsilon_0 b}\left\{\frac{b}{c}\omega-\frac{1}{3!}\left(\frac{b}{c}\right)^3\omega^3+\frac{1}{5!}\left(\frac{b}{c}\right)^5\omega^5-\cdots\right\}\\&=-\frac{\mu_0}{4\pi}\left\{c\omega-\frac{1}{3!}\frac{b^2}{c}\omega^3+\frac{1}{5!}\frac{b^4}{c^3}\omega^5-\cdots\right\},\end{aligned} \tag{26}$$

$$P_{12}^{\mathrm{j}} = -\frac{\sin(\omega\frac{D}{c})}{4\pi\varepsilon_0 D}$$
$$= -\frac{1}{4\pi\varepsilon_0 D}\left\{\frac{D}{c}\omega - \frac{1}{3!}\left(\frac{D}{c}\right)^3\omega^3 + \frac{1}{5!}\left(\frac{D}{c}\right)^5\omega^5 - \cdots\right\}$$
$$= -\frac{\mu_0}{4\pi}\left\{c\omega - \frac{1}{3!}\frac{D^2}{c}\omega^3 + \frac{1}{5!}\frac{D^4}{c^3}\omega^5 - \cdots\right\}. \quad (27)$$

Using Eqs. (25), (26), and (27), we express Z^{r} as the function of ω:

$$Z^{\mathrm{r}} = \frac{\mu_0}{4\pi}\left\{\left(\frac{2D^2+b^2}{3c}\right)\omega^2 - \left(\frac{2D^4+30D^2a^2+3b^4}{180c^3}\right)\omega^4\cdots\right\}. \quad (28)$$

The radiation resistance of the Hertzian dipole is expressed as [16]

$$R_r = \frac{\mu_0\omega^2D^2}{6\pi c}. \quad (29)$$

Because we assume that $b \ll D$, the term, ω^2 in Eq. (28) approximates the radiation resistance, R_{r} in Eq. (29). Thus, the equivalent-circuit model with electromagnetic retardation expresses the radiation loss.

3.3 Comparison with Electromagnetic Simulation

We analyze the frequency response of the current of a wire in the I-shaped meta-atom having the parameters, $a = 0.01$ mm, $b = 1$ mm, and $D = 7$ mm. The direction of the electromagnetic field and the result are shown in Fig. 5. The wire between two spheres is excited by a linearly polarized plane wave, $E^{\mathrm{E}} = 1$V/m. In order to specify the effect of the retardation, we show the result of the model without the retardation together. Because the model without the retardation is a lossless circuit, the amplitude at the resonance frequency goes to infinity.

We use MWstudio® for the electromagnetic simulations. The MWstudio® electromagnetic-field analysis uses the finite integration technique (FIT). The relative difference of the resonant frequencies and quality factor between the proposed model and FIT are 3.0% and 3.8% respectively. The main errors of the results come from the condition $D \ll \lambda$ between the distance D of the spheres and the wavelength λ of the incident wave. However, it is noted that the results from the proposed model are obtained by the very simple model Eq. (21).

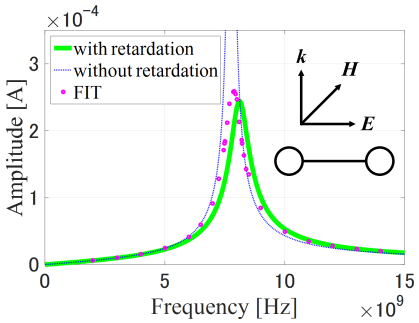

Fig. 5 Frequency response of the current, I_1.

4. Retarded Electromagnetic Coupling

4.1 Mode Decomposition of the Circuit Equation

To clarify the retarded electromagnetic coupling, we analyze two coupled I-shaped meta-atoms, as shown in Fig. 6. Matrix $\hat{\boldsymbol{L}}$ of the coupled meta-atoms is expressed as

$$\hat{\boldsymbol{L}}(\omega) = \begin{bmatrix}\hat{L} & \hat{M}\\ \hat{M} & \hat{L}\end{bmatrix}. \quad (30)$$

The self-inductance, $\hat{L}$, is expressed in Eq. (18). The mutual inductance, $\hat{M}$, is expressed as

$$\hat{M} = \frac{\mu_0}{4\pi}\int_0^D\int_0^D \frac{\exp(-\mathrm{j}\omega\frac{\sqrt{(z-z')^2+h^2}}{c})}{\sqrt{(z-z')^2+h^2}}\mathrm{d}z'\mathrm{d}z \quad (31)$$
$$\simeq \exp\left(-\mathrm{j}\omega\frac{h}{c}\right)\frac{\mu_0 D}{2\pi}\left\{\log\left(\alpha+\sqrt{1+\alpha^2}\right) - \sqrt{1+\frac{1}{\alpha^2}} + \frac{1}{\alpha}\right\}, \quad (32)$$

where $\alpha = \frac{D}{h}$. $\hat{M}$ is also a complex number and depends on the frequency. Matrix $\hat{\boldsymbol{P}}$ is expressed as

$$\hat{\boldsymbol{P}}(\omega) = \begin{bmatrix}\hat{P}_{11} & \hat{P}_{12} & \hat{P}_{13} & \hat{P}_{14}\\ \hat{P}_{21} & \hat{P}_{22} & \hat{P}_{23} & \hat{P}_{24}\\ \hat{P}_{31} & \hat{P}_{32} & \hat{P}_{33} & \hat{P}_{34}\\ \hat{P}_{41} & \hat{P}_{42} & \hat{P}_{43} & \hat{P}_{44}\end{bmatrix}, \quad (33)$$

where

$$\hat{P}_{11} = \hat{P}_{22} = \hat{P}_{33} = \hat{P}_{44} = \frac{\exp(-\mathrm{j}\omega\frac{b}{c})}{4\pi\varepsilon_0 b}, \quad (34)$$
$$\hat{P}_{12} = \hat{P}_{21} = \hat{P}_{34} = \hat{P}_{43} = \frac{\exp(-\mathrm{j}\omega\frac{D}{c})}{4\pi\varepsilon_0 D}, \quad (35)$$
$$\hat{P}_{13} = \hat{P}_{31} = \hat{P}_{24} = \hat{P}_{42} = \frac{\exp(-\mathrm{j}\omega\frac{h}{c})}{4\pi\varepsilon_0 h}, \quad (36)$$
$$\hat{P}_{14} = \hat{P}_{41} = \hat{P}_{23} = \hat{P}_{32} = \frac{\exp(-\mathrm{j}\omega\frac{\sqrt{D^2+h^2}}{c})}{4\pi\varepsilon_0\sqrt{D^2+h^2}}. \quad (37)$$

The incident matrix, $\boldsymbol{U}$, is expressed as

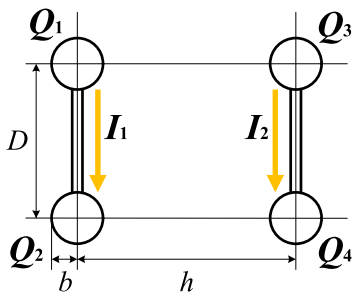

Fig. 6 Coupled meta-atoms.

$$\boldsymbol{U} = \begin{bmatrix} -1 & 0 \\ 1 & 0 \\ 0 & -1 \\ 0 & 1 \end{bmatrix}. \tag{38}$$

In order to decompose the equivalent-circuit equation, we define $\hat{\boldsymbol{F}} \equiv \hat{\boldsymbol{L}}^{-1}\boldsymbol{U}^{\mathrm{T}}\hat{\boldsymbol{P}}\boldsymbol{U}$ in Eq. (13).

Because the coupled meta-atoms have even and odd modes, if we define the mode decomposition matrix, $\boldsymbol{K}$, as

$$\boldsymbol{K} \equiv \frac{1}{\sqrt{2}}\begin{bmatrix} 1 & 1 \\ 1 & -1 \end{bmatrix}, \tag{39}$$

we can diagonalize the left-side of Eq. (13) as

$$\begin{aligned}&(-\omega^2\mathbf{1} + \hat{\boldsymbol{K}}^{-1}\hat{\boldsymbol{F}}\hat{\boldsymbol{K}})\hat{\boldsymbol{K}}^{-1}\boldsymbol{I}(\omega) \\ &= \left\{-\omega^2\begin{bmatrix} 1 & 0 \\ 0 & 1 \end{bmatrix} + \begin{bmatrix} \hat{\lambda}_{\mathrm{even}}(\omega) & 0 \\ 0 & \hat{\lambda}_{\mathrm{odd}}(\omega) \end{bmatrix}\right\}\begin{bmatrix} I_{\mathrm{even}}(\omega) \\ I_{\mathrm{odd}}(\omega) \end{bmatrix},\end{aligned} \tag{40}$$

where

$$\hat{\lambda}_{\mathrm{even}}(\omega) = \frac{\hat{P}^{\mathrm{s}} + \hat{P}^{\mathrm{m}}}{2\pi\varepsilon_0(\hat{L} + \hat{M})}, \quad \hat{\lambda}_{\mathrm{odd}}(\omega) = \frac{\hat{P}^{\mathrm{s}} - \hat{P}^{\mathrm{m}}}{2\pi\varepsilon_0(\hat{L} - \hat{M})}, \tag{41}$$

and

$$\hat{P}^{\mathrm{s}} = \frac{\exp(-\mathrm{j}\omega\frac{b}{c})}{b} - \frac{\exp(-\mathrm{j}\omega\frac{D}{c})}{D}, \tag{42}$$

$$\hat{P}^{\mathrm{m}} = \frac{\exp(-\mathrm{j}\omega\frac{h}{c})}{h} - \frac{\exp(-\mathrm{j}\omega\frac{\sqrt{D^2+h^2}}{c})}{\sqrt{D^2+h^2}}. \tag{43}$$

Because eigenvalues, $\hat{\lambda}_{\mathrm{even}}$ and $\hat{\lambda}_{\mathrm{odd}}$, are functions of ω, the natural angular frequencies of the even mode, ω_{even} and those of the odd mode, ω_{odd}, are calculated by solving

$$-\omega^2 + \hat{\lambda}_{\mathrm{even}}(\omega) = 0, \quad -\omega^2 + \hat{\lambda}_{\mathrm{odd}}(\omega) = 0, \tag{44}$$

respectively.

4.2 Natural Angular Frequencies of the Retarded Coupling

The two natural angular frequencies are complex numbers and are expressed as

$$\omega_{\mathrm{even}} = \omega^{\mathrm{r}}_{\mathrm{even}} + \mathrm{j}\omega^{\mathrm{j}}_{\mathrm{even}}, \quad \omega_{\mathrm{odd}} = \omega^{\mathrm{r}}_{\mathrm{odd}} + \mathrm{j}\omega^{\mathrm{j}}_{\mathrm{odd}}. \tag{45}$$

The distance, h, dependencies of the real and imaginary parts of the ω_{even} and ω_{odd} are shown in Figs. 7 and 8, respectively. The real parts in Fig. 7 show that the frequency of $\omega^{\mathrm{r}}_{\mathrm{even}}$ and $\omega^{\mathrm{r}}_{\mathrm{odd}}$ changes, depending upon h. $\omega^{\mathrm{r}}_{\mathrm{even}}$ and $\omega^{\mathrm{r}}_{\mathrm{odd}}$ have certain cross points and the coupling between the two meta-atoms are neutralized at these cross points. Because the distances between the cross points are approximately 20 mm, which is half the wavelength, the sign of the coupling between the two meta-atoms changes periodically. The cross points in Fig. 7 correspond to the maximal and minimum points in Fig. 8, demonstrating the relationship between the coupling and radiation loss. That is, the effects of the mutual coupling in the eigenvalues in Eq. (41) are represented by the $\hat{M}$ and $\hat{P}_{\mathrm{m}}$, and both the $\hat{M}$ by Eq. (32) and $\hat{P}_{\mathrm{m}}$ by Eq. (43) have h dependency of $\exp(-\mathrm{j}\omega\frac{h}{c})$ and $\exp(-\mathrm{j}\omega\frac{\sqrt{D^2+h^2}}{c})$ on the complex plane. As a result, the resonant frequencies and radiation losses which correspond to the real and imaginary parts of the natural angular frequencies have such relationship in h dependencies.

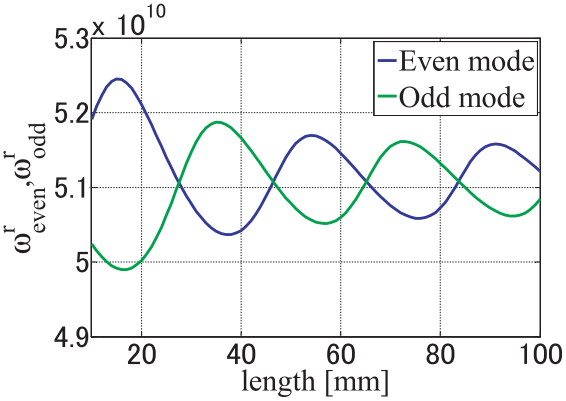

Fig. 7 h dependencies of the real parts, $\omega^{\mathrm{r}}_{\mathrm{even}}$ and $\omega^{\mathrm{r}}_{\mathrm{odd}}$, with retardation.

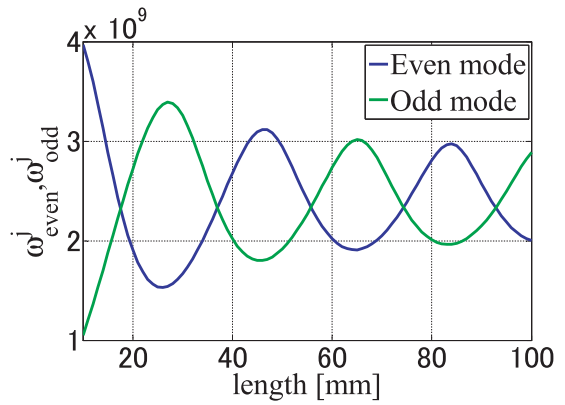

Fig. 8 h dependencies of the imaginary parts, $\omega^{\mathrm{j}}_{\mathrm{even}}$ and $\omega^{\mathrm{j}}_{\mathrm{odd}}$, with retardation.

4.3 Natural Angular Frequencies without Retardation

In order to estimate the effect of retarded coupling, we display the results of the model without retardation, in Fig. 9. The natural angular frequencies, ω_{even} and ω_{odd}, have only real parts, $\omega^{\mathrm{r}}_{\mathrm{even}}$ and $\omega^{\mathrm{r}}_{\mathrm{odd}}$ because the inductances and potential coefficients are not complex numbers, without retardation. $\omega^{\mathrm{r}}_{\mathrm{odd}}$ is always greater than $\omega^{\mathrm{r}}_{\mathrm{even}}$ and they approach each other, as the distance, h, increases. Thus, the sign of the coupling between the two meta-atoms does not change, when the retardation is neglected.

4.4 Electromagnetic Field Analysis

In order to confirm the existence of cross points in Fig. 7,

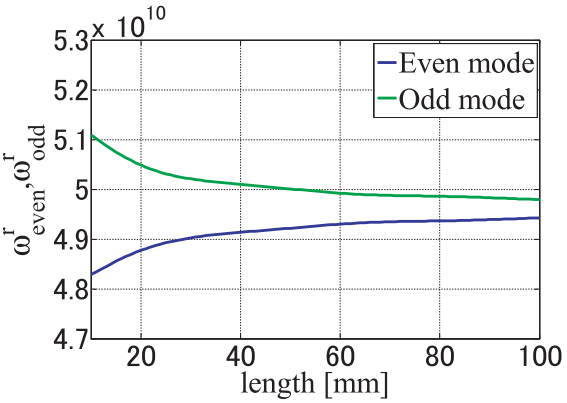

Fig. 9 h dependencies of the real parts, ω^{r}_{even} and ω^{r}_{odd}, without retardation.

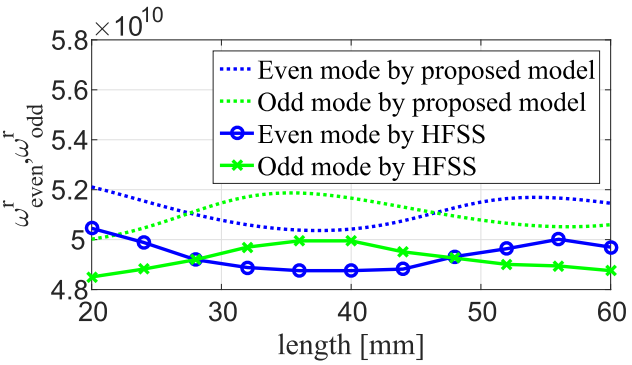

Fig. 10 Comparison of h dependencies of the real parts, ω^{r}_{even} and ω^{r}_{odd}, by electromagnetic simulation with ANSYS HFSS.

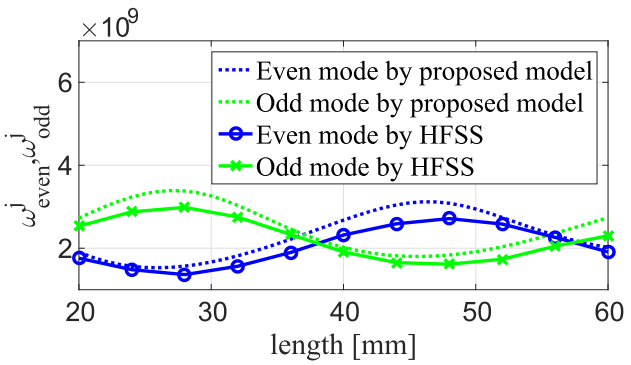

Fig. 11 Comparison of h dependencies of the imaginary parts, ω^{j}_{even} and ω^{j}_{odd}, by electromagnetic simulation with ANSYS HFSS.

we calculate ω_{even} and ω_{odd} by eigenmode analysis using ANSYS HFSS. ω_{even} and ω_{odd} obtained by electromagnetic-field analysis are shown in Figs. 10 and 11, respectively. The maximum relative differences between the proposed model and HFSS are 3.9% in Fig. 10 and 15% in Fig. 11, respectively. The large differences in the imaginary parts are due to the small imaginary parts compared to the real parts. From Fig. 10, it is confirmed that the frequency ω^{r}_{even} and ω^{r}_{odd} is reversed at $h = 28$ mm and $h = 48$ mm. From Fig. 11, the cross points in Fig. 10 correspond to the maximum and minimum points. Although the average values of the even and odd modes of the model without the retardation in Fig. 9 give a better approximation of those in Fig. 10, the model without the retardation does not have the cross points. Thus, both the proposed model and the electromagnetic-field analysis agree in that there exist cross points in h dependency.

5. Conclusion

A simple equivalent-circuit model with retardation, for wired metallic spheres, was proposed in this paper and the effects of retarded electromagnetic coupling in simple meta-atoms were clarified.

Retardation renders the inductances and potential coefficients complex numbers. It was demonstrated that the imaginary components in the proposed model correspond to the radiation loss. The formulation provides consistent equivalent circuits only at the near-field without the radiation estimation calculated at the far-field.

Further, the retarded electromagnetic coupling of two meta-atoms renders the natural angular frequencies of the even and odd modes complex numbers; the magnitude relationship between the two natural angular frequencies varies, depending upon the distance, h. Thus, the proposed model suggests that retarded electromagnetic coupling impacts the modeling of the radiation and the coupling of meta-atoms.

References

[1] N. Engheta, "Circuits with light at nanoscales: Optical nanocircuits inspired by metamaterials," Science, vol.317, no.5845, pp.1698–1702, Sept. 2007.

[2] J.D. Baena, J. Bonache, F. Martín, R.M. Sillero, F. Falcone, T. Lopetegi, M.A.G. Laso, J. G-García, I. Gil, M.F. Portillo, and M. Sorolla, "Equivalent-circuit models for split-ring resonators and complementary split-ring resonators coupled to planar transmission lines," IEEE Trans. Microw. Theory Techn., vol.53, no.4, pp.1451–1461, April 2005.

[3] F. Bilotti, A. Toscano, L. Vegni, K. Aydin, K.B. Alici, and E. Ozbay, "Equivalent-circuit models for the design of metamaterials based on artificial magnetic inclusions," IEEE Trans. Microw. Theory Techn., vol.55, no.12, pp.2865–2873, Dec. 2007.

[4] M. Shamonin, E. Shamonina, V. Kalinin, and L. Solymar, "Properties of a metamaterial element: Analytical solutions and numerical simulations for a singly split double ring," J. Appl. Phys., vol.95, no.7, pp.3778–3784, April 2004.

[5] A. Alù and S. Maslovski, "Power relations and a consistent analytic model for receiving wire antennas," IEEE Trans. Antennas Propag., vol.58, no.5, pp.1436–1448, May 2010.

[6] I. Liberal and R.W. Ziolkowski, "Analytical and equivalent circuit models to elucidate power balance in scattering problems," IEEE Trans. Antennas Propag., vol.61, no.5, pp.2714–2726, May 2013.

[7] A.E. Ruehli and A.C. Cangellaris, "Progress in the methodologies for the electrical modeling of interconnects and electronic packages," Proc. IEEE, vol.89, no.5, pp.740–771, May 2001.

[8] M.E. Verbeek, "Partial element equivalent circuit (PEEC) models for on-chip passives and interconnects," Int. J. Numer. Model., vol.17, no.1, pp.61–84, 2004.

[9] T. Hisakado, K. Yoshida, T. Matsushima, and O. Wada, "Equivalent-circuit model for Meta-Atoms Consisting of Wired Metallic Spheres," IEICE Trans. Electronics, vol.E100-C, no.3, pp.305–312, 2017.

[10] A. Sanada, "Characteristics of an isotropic 3-dimensional left-handed metamaterial composed of wired metallic spheres," IEICE Electron. Express, vol.6, no.11, pp.689–702, 2009.
[11] H. Heeb and A.E. Ruehli, "Three-Dimensional Interconnect Analysis Using Partial Element Equivalent Circuits," IEEE Trans. Circuits and Systems, vol.39, no.11, pp.974–982, Nov. 1992.
[12] R. Taubert, M. Hentschel, J. Kästel, and H. Giessen, "Classical Analog of Electromagnetically Induced Absorption in Plasmonics," Nano Lett., vol.12, pp.1367–1371, 2012.
[13] H. Toki and K. Sato, "Alternating current circuit theory with antenna process and the reduction of electromagnetic noise," J. Phys. Soc. Jpn. Suppl., vol.68, no.1, pp.11–18, Jan. 2013.
[14] L.K. Yeung and K.-L. Wu, "Generalized Partial Element Equivalent Circuit (PEEC) Modeling with Radiation Effect," IEEE Trans. Microw. Theory Techn., vol.59, no.10, pp.2377–2384, Oct. 2011.
[15] Y.S. Cao, L.J. Jiang, and A.E. Ruehli, "Distributive Radiation and Transfer Characterization Based on the PEEC Method," IEEE Trans. Electromagn. Compat., vol.57, no.4, pp.734–742, Aug. 2015.
[16] L. Solymar and E. Shamonina, "Waves in metamaterials," chap. 1, pp.1–33, OXFORD, 2014.

Appendix A: Calculation of the Self-Inductance with Retardation

From Eq. (14), the real part of the self-inductance, $\mathrm{Real}\left\{\hat{L}_{nn}\right\}$, is expressed as

$$\mathrm{Real}\left\{\hat{L}_{nn}\right\} = \mu_0 \int_V \int_{V'} \boldsymbol{\Psi}_n^{\mathrm{S}}(\boldsymbol{r}) \frac{\cos(\omega\frac{|\boldsymbol{r}-\boldsymbol{r}'|}{c})}{4\pi|\boldsymbol{r}-\boldsymbol{r}'|} \boldsymbol{\Psi}_{n'}(\boldsymbol{r}')\mathrm{d}^3\boldsymbol{r}'\mathrm{d}^3\boldsymbol{r}. \quad (\mathrm{A}\cdot 1)$$

Assuming that $\cos(\omega\frac{|\boldsymbol{r}-\boldsymbol{r}'|}{c}) \simeq 1$, Eq. (A·1) is approximated by

$$\mathrm{Real}\left\{\hat{L}_{nn}\right\} \simeq \mu_0 \int_V \int_{V'} \boldsymbol{\Psi}_n^{\mathrm{S}}(\boldsymbol{r}) \frac{1}{4\pi|\boldsymbol{r}-\boldsymbol{r}'|} \boldsymbol{\Psi}_{n'}(\boldsymbol{r}')\mathrm{d}^3\boldsymbol{r}'\mathrm{d}^3\boldsymbol{r}. \quad (\mathrm{A}\cdot 2)$$

Because $\mathrm{Real}\left\{\hat{L}_{nn}\right\}$ depends on the function $\frac{1}{|\boldsymbol{r}-\boldsymbol{r}'|}$, the thin wire-part of the meta-atom is dominant for $\mathrm{Real}\left\{\hat{L}_{nn}\right\}$ and we use the test function $\boldsymbol{\Psi}_n^{\mathrm{S}}(\boldsymbol{r})$, which exists only on the wire, for the calculation of the self-inductance in Eq. (4); i.e., we calculate $\mathrm{Real}\left\{\hat{L}_{nn}\right\}$ as

$$\mathrm{Real}\left\{\hat{L}_{nn}\right\} \simeq \frac{\mu_0}{4\pi} \int_b^{D-b} \int_0^D \frac{\cos(\omega\frac{\sqrt{(z-z')^2+a^2}}{c})}{\sqrt{(z-z')^2+a^2}} \mathrm{d}z'\mathrm{d}z. \quad (\mathrm{A}\cdot 3)$$

On the other hand, the imaginary part, $\mathrm{Imag}\left\{\hat{L}_{nn}\right\}$, is expressed as

$$\mathrm{Imag}\left\{\hat{L}_{nn}\right\} = \mu_0 \int_V \int_{V'} \boldsymbol{\Psi}_n^{\mathrm{S}}(\boldsymbol{r}) \frac{\sin(\omega\frac{|\boldsymbol{r}-\boldsymbol{r}'|}{c})}{4\pi|\boldsymbol{r}-\boldsymbol{r}'|} \boldsymbol{\Psi}_{n'}(\boldsymbol{r}')\mathrm{d}^3\boldsymbol{r}'\mathrm{d}^3\boldsymbol{r}. \quad (\mathrm{A}\cdot 4)$$

Assuming that $\sin(\omega\frac{|\boldsymbol{r}-\boldsymbol{r}'|}{c})$ is sufficiently small, we can use the approximation

$$\sin(\omega\frac{|\boldsymbol{r}-\boldsymbol{r}'|}{c}) \simeq \omega\frac{|\boldsymbol{r}-\boldsymbol{r}'|}{c}. \quad (\mathrm{A}\cdot 5)$$

Hence, Eq. (A·4) is approximated by

$$\mathrm{Imag}\left\{\hat{L}_{nn}\right\} \simeq \mu_0 \int_V \int_{V'} \boldsymbol{\Psi}_n^{\mathrm{S}}(\boldsymbol{r}) \frac{\omega}{4\pi c} \boldsymbol{\Psi}_{n'}(\boldsymbol{r}')\mathrm{d}^3\boldsymbol{r}'\mathrm{d}^3\boldsymbol{r}. \quad (\mathrm{A}\cdot 6)$$

Because $\mathrm{Imag}\left\{\hat{L}_{nn}\right\}$ does not depend on the function $\frac{1}{|\boldsymbol{r}-\boldsymbol{r}'|}$, we have to consider the sphere-part in addition to the wire-part. As a result, we calculate $\mathrm{Imag}\left\{\hat{L}_{nn}\right\}$ adopting the length, D, as the interval of integration, similar to the mutual inductances. Therefore, $\mathrm{Imag}\left\{\hat{L}_{nn}\right\}$ is calculated as

$$\mathrm{Imag}\left\{\hat{L}_{nn}\right\} \simeq \frac{\mu_0}{4\pi} \int_0^D \int_0^D \frac{\sin(\omega\frac{\sqrt{(z-z')^2+a^2}}{c})}{\sqrt{(z-z')^2+a^2}} \mathrm{d}z'\mathrm{d}z. \quad (\mathrm{A}\cdot 7)$$

Katsuya Ohishi received his M.E. degree in Electrical Engineering from Kyoto University, Kyoto Japan, in 2016. His research interest is introducing the equivalent circuit model for electromagnetic phenomena in metamaterials.

Takashi Hisakado Received the B.E., and M.E., degrees in Electrical Engineering II from Kyoto University, in 1993 and 1995, respectively. He received the Dr. degree in Electrical Engineering from Kyoto University, in 1997. He is currently Associate Professor of Department of Electrical Engineering at Kyoto University. His research interests are design of electromagnetic phenomena and power flow. He is a member of IEEJ and IEEE.

Tohlu Matsushima received his M.E. and Ph.D. degrees in Communication Network Engineering from Okayama University in 2006 and 2009, respectively. From 2009, he was an assistant professor in Department of Electrical Engineering at Kyoto University from 2009. His research interest is electromagnetic interference problem. He is a member of IEEE, the Institute of Electrical Engineers of Japan (IEEJ), and the Japan Institute of Electronics Packaging (JIEP).

Osami Wada received the B.E., M.E., and Dr. Eng. degrees in Electronics from Kyoto University in 1981, 1983, and 1987, respectively. From 1988 to 2005, he was in the Faculty of Engineering, Okayama University, Japan. In 2005, he became a Full Professor in the Department of Electrical Engineering at Kyoto University. He has been engaged in the study of electromagnetic compatibility (EMC) of electronic circuits and systems, and development of EMC macromodels of integrated circuits. Prof. Wada is a member of IEEE, the Institute of Electrical Engineers of Japan (IEEJ), and the Japan Institute of Electronics Packaging (JIEP). He is a Fellow of the IEICE.